ORIGINAL STUDY

Application of seismic refraction and MASW methods for investigating the Spillway Fault trace along the western side of the Aswan High Dam, Egypt

Ahmed Hamed[1] · Raafat El-Shafie Fat-Helbary[1] · Abdel-Monem Mohamed[1] · Karrar Omar El-Faragawy[2] · Ahmed Abd El Gaber[2] · Ahmed M. Meneisy[2]

Abstract

An earthquake of local magnitude $M_L = 4.6$ occurred on November 7, 2010, 4.5 km northwest of the Aswan High Dam on the Spillway Fault. In the Aswan metropolitan region this earthquake was felt intensely. As no surface rupture was found, the focal mechanism and the distribution of seismic activity was one of the tools used for finding fault dimensions. The composite fault-plane solutions for the observed events on the Spillway Fault showed a left lateral strike-slip faulting with normal-fault component striking NNW-SSE. Also, remote sensing techniques were applied for the detection and identification of the geomorphology and geometry of the Spillway Fault. In this research, sub-surface layers and structures are delineated utilizing near-surface seismic techniques. Furthermore, the area's supposed path and position of the Spillway Fault are also investigated. Two active seismic techniques, Seismic Refraction and Multi-Channel Analysis of Surface Waves (MASW), are utilized for recording near-surface seismic wave data at 9 sites. The seismic refraction profiles are conducted as a 2D cross-section on the trace of the detected Spillway Fault in the study area to evaluate the maximum depth of penetration of the P-wave for fault investigation. The constructed 2D seismic and structural sections from P-wave results show that the obtained average depth of about 30 m. In addition, the estimated P-wave velocities extend from 600 m/s to over 6500 m/s. Some lateral variation in the seismic wave velocities in all layers may represent fault zones. Moreover, the 1D MASW technique is conducted to estimate the velocities of the shear wave for the upper 30 m (Vs30) to provide the site classes and soil characteristics along both sides of the detected Spillway Fault trace in the study area. The calculated Vs30 values emphasized the idea of the existence of a normal dip-slip fault trace which divides the study area into two different lithological parts. The first part is located on the eastern side and characterized by almost class B (hard rock, according to NEHRP classification), while the other part is located to the west, and shows almost class type C (denoted as dense soil and soft rock soil).

✉ Ahmed M. Meneisy
ahmedmeneisy@sci.aswu.edu.eg

1 National Research Institute of Astronomy and Geophysics, Cairo 11421, Egypt

2 Department of Geology, Faculty of Science, Aswan University, Aswan 81528, Egypt

1 Introduction

On November 7, 2010, an earthquake of magnitude $M_L = 4.6$ according to the Richter scale took place in Aswan area, Upper Egypt. This earthquake was felt by the locals. This earthquake was located in the middle area about 4.5 km west of the High and Old Aswan Dams (Fig. 1), and observed by Aswan and Egyptian National Seismic Networks as in Table 1, This earthquake is moderate, while its importance comes from its proximity to the High and Old Aswan Dams' sites and to the Aswan residential areas (Dahy 2012; Fat-Helbary et al. 2012; Mohamed et al. 2022; El-Bohoty et al. 2023).

The focal mechanism and the spread of seismic activity were two methods utilized before for determining fault size since no surface rupture was discovered at the epicentre of the earthquake. The composite fault-plane solutions for the observed events on the Spillway Fault showed a left lateral strike-slip faulting with normal-fault component striking NNW-SSE (El-Bohoty et al. 2023). Remote sensing techniques were also applied for the detection and identification of the geomorphology and geometry of Spillway Fault, and lineament extraction. Two shallow seismic methods—Shallow Seismic Refraction (SSR) and Multi-Channel Analysis of Surface Waves (MASW)—were used in this study to
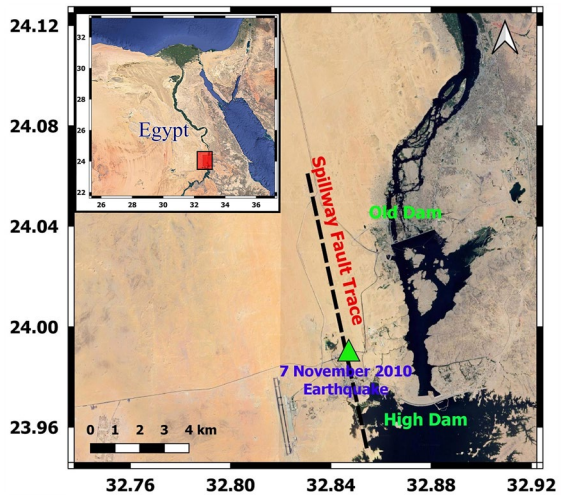

Fig. 1 Location map of the study area

Table 1 The earthquake parameters

Date	Origin Time			Location		Depth	Magnitude
	hour	minute	second	Latitude °N	Longitude °E		
7/11/2010	09	54	34.15	24.0	32.85	2 km	4.6

identify the subsurface structures and layers as well as to look into the suspected path and position of the Spillway Fault in the region.

One of the most useful geophysical techniques is known as shallow seismic refraction (SSR), which can be used to identify the depth of the bedrock, and geotechnical parameters of the investigated sites (Meneisy et al. 2020; 2023; Fat-Helbary et al. 2019b), the depth to the water table (Butler 1990; Holzer and Bennett 2003; Burger et al. 2006), the kind of lithology, the lateral and vertical changes in lithology (Al-Heety and Shanshal 2016), in addition to, investigate the probable subsurface structural features like faults and cracks (Karastathis et al. 2006; Hamed 2019; Rasif et al. 2023). In order to conduct a seismic refraction survey, field data must be collected, processed, and interpreted. For accurate data acquisition and interpretation, the application of geologic information of the studied area is implied. On the other hand, data processing which includes both the construction and inversion of travel time curves does not require geologic information. The Shallow seismic refraction survey was conducted as a cross-section profiles on the supposed path and location of the Spillway Fault in the study area.

Multi-Channel Analysis of Surface Waves (MASW) technique has been applied to classify the uppermost part of the surface layers of the study area (Park et al. 1999). The dispersive property of Rayleigh waves as they travel across a stratified material forms the cornerstone of surface wave approaches. Dispersion is the term used to describe how phase velocity varies with frequency (Rahnema et al. 2020). The relevant Vs profile is back-calculated from the obtained dispersion curve using iterative forward or inverse modeling approaches, then it is possible to determine Vs30 from the acquired Vs profile (Al-Heety and Shanshal 2016; and Hamed et al. 2023). Shear-wave velocity, according to Bessason and Erlingsson (2011), Toni (2012), Toni et al. (2019, 2022) and Meneisy et al. (2020) is a crucial factor in estimating a soil layer's stiffness. Hence, increases in material shear strength or rigidity are a result of the shear-wave velocity increasing (Ivanov et al. 2008). There are already a number of international classification codes that categorize locations depending on the vertical shear wave velocity measurements. The seismic classification schemes offered by the National Earthquake Hazard Reduction Program (NEHRP system) are employed in this study (Table 2).

Table 2 NEHRP seismic site classification based on shear wave

Site Class	Description	Average shear wave velocity (m/s) top 30 m
A	Hard rock	$Vs30_{avg} > 1500$
B	Rock	$760 < Vs30_{avg} \leq 1500$
C	Very dense soil	$360 < Vs30_{avg} \leq 760$
D	Stiff soil	$180 \leq Vs30_{avg} \leq 360$
E	Soft soil	$Vs30_{avg} < 180$
F	Soils requiring site-specific evaluation	–

2 Local geology of the study area

The geological setting of the Aswan High Dam area (Fig. 2a) is mainly consists of the Cretaceous Nubian Sandstone formation belonging to the upper Cretaceous which located above Precambrian crystalline hard igneous and metamorphic rocks (EGSMA 2002). The sandstone succession covered most places in the study area with thickness ranges between 70 and 162 m. On the other hand, this thickness shrinks to about 30 m in proximity to the spillway emergency bridge (Fig. 2b), while the basement rocks appear at some places near or on the surface. The successions of the Nubian sandstone group consist of several formations, namely Umm Barmil, Timsah, and Abu Aggag Formations. Most of these formations consist of clastic deposits of sandstone and shale, but the Timsah Formation is characterized by the presence of layers of Oolitic iron ore, which was exploited in the Abu Aggag area east of the Nile River. The rocks of these units are characterized by the horizontal and vertical change in sedimentary facies from sandstone to alluvial deposits and shale. The thickness of the Umm Barmil Formation is about 40 m. It consists of
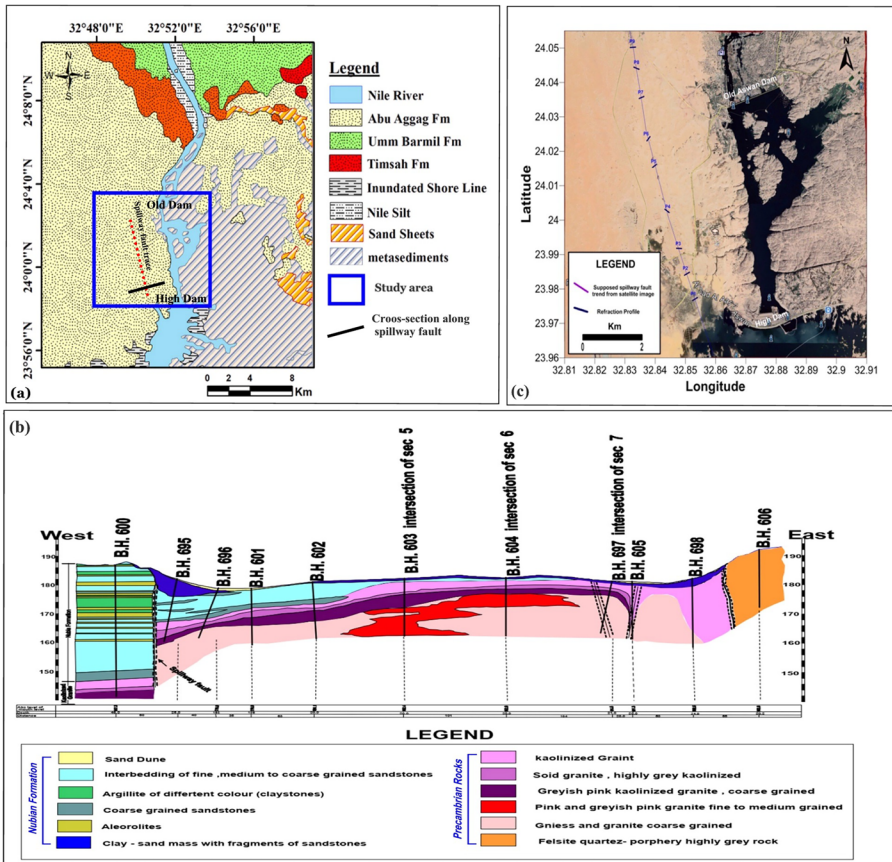

Fig. 2 Geological map of the Aswan High Dam area (after EGSMA 2002) (**a**), cross-section along spillway fault (WCC,1985) (**b**), and the location map for the seismic refraction profiles along the Supposed spillway fault trace (**c**)

coarse-to-medium-grained sandstone with the presence of the phenomenon of the primary stratigraphic intersection with intrusions of the silt. The Umm Barmil Formation is located above the Timsah Formation with an erosion surface. The Timsah Formation thickness ranges from 10 and 35 m and consists of sandstone and kaolinitic silt with the presence of some overlaps of iron oxides. There is a Timsah Formation on top of the Abu Aggag Formation with a surface of unconformity. While the Abu Aggag Formation thickness ranges from 30 and 40 m. It consists of coarse-grained non-graded kaolin sandstone which characterizes the channels of sedimentation. According to Attia (1955); Hendriks et al. (1987); Youssef (2003) the Abu Aggag Formation is located in the Aswan region directly above the basement rocks with the presence of unconformity surfaces (Fig. 2b).

3 Methodology

3.1 Shallow seismic refraction

In seismic refraction, it is important to remember that the subsurface is made up of a sequence of layers separated by planes of dipping surfaces. Seismic velocities are also consistent inside each layer, and layer's velocity increases with depth, constraining ray paths to the vertical plane containing the profile line (Adeoti et al. 2012). The seismic refraction method uses a variety of sensors evenly distributed along a survey line to track the elastic compression wave as it travels through geological material. For deep prospection, elastic waves can also be induced at the middle and the two terminals of the survey line by mass falls, hammers, or explosives. When the elastic wave reaches its location, sensors known as geophones monitor the vibration velocity, which allows them to detect these waves. The needed depth of investigation determines the dimension of the survey line and the distance between detectors. The space–time curves are then constructed by using the data to figure out the time at which the compression waves arrive at each geophone. The seismic profile can be established by analyzing these curves (Kearey et al. 2002).

In the current investigation, the field collection procedure for data started with a site investigation to map out traverses (profiles), during which data were collected using a vertical geophone with a natural frequency of 14 Hz and a seismograph with 48 channels, the modal is Strata Visor-NZ. Nine profiles have been conducted in this investigation, distributed perpendicular to the supposed trace of the Spillway Fault, which is displayed on the base map as solid blue lines (Fig. 2c). The source energy needed for such a relatively near surface investigation has been supplied using a thick and heavy metallic plate and a sledge hammer weighing around 10 kg. Along the profile into the earth, the geophones are properly set vertically. To improve ground connection and the ability to detect seismic waves, spike geophones were buried in the ground. There are 24 geophones set up with a constant distance of 5 m between them and an overall spread of 115 m. The data was gathered with a 0.25 ms sampling period (interval) and a 0.75 s total recording time length. The front, center, and reverse firing techniques were used to collect the data and produce the P-wave (Fig. 3a). An example of a field seismic survey in the research area is shown in (Fig. 3b).

First picks for the frontal, center, and backward firing were selected from stored data files after being visually examined and checked for accuracy (Fig. 4a). To create a set of travel time-distance curves for every line, the chosen initial arrival times were plotted against the source-to-geophone intervals (Fig. 4b). Following checking for compatibility using the intercept-time principles, these traveltime-distance curves were some of them

Fig. 3 Configuration of the seismic refraction survey with shot location and geophone spreading (**a**), photo of the field survey (**b**)

rectified for accurate data explanation. An efficient 2D tomographic inversion method was used to analyze and explain the plotted time-distance graphs of the gathered data (GODO-GRAF software). Moscow State University created the program that we are using (Piip 1991, 2001). In this system, every couple of reversed traveltime curves chosen from the entire set of curves has the homogeneous function fitted to the real velocity section. From the simplest instance of two inverted traveltime curves to situations where the receivers and sources are evenly dispersed throughout the profile, the inversion is appropriate to any combination of traveltime curves (Piip 2001). Building a seismic section as a 2D velocity model is made possible by inversion (Fig. 4c). This model is indeed a seismic cross-section, where the resultant velocity field values are calculated at vertices of a grid pattern and they are shown as a field of velocity contour lines with a constant interval. Those seismic models have the potential to include straight-lined seismic barriers (lines of function discontinuity), where the velocity gradient is irregular (as seen in Fig. 4c).

In contrast, the identical velocity field is shown in the structural sections as a surface with shaded relief that is overlaid by velocity contour isolines. The obtained gradient is inversely proportional to the space between contours, it is feasible to visually estimate
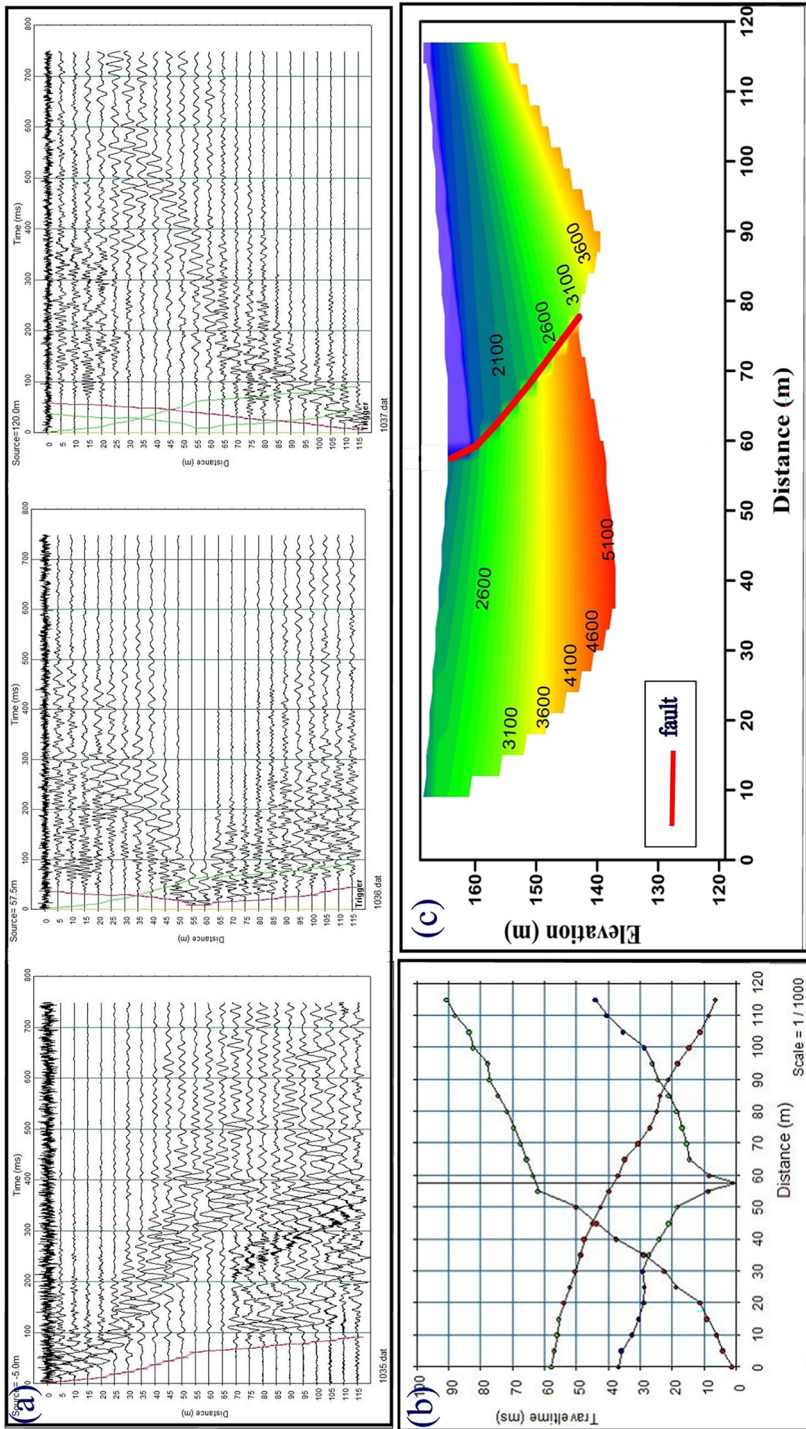
Fig. 4 Steps of shallow seismic refraction processing; forward, middle, and reverse shootings (**a**); travel-time distance curve (**b**) and 2D velocity model (**c**) (ex. Profile No.6)

the velocity gradient values from these lines (Piip 2001; Piip and El-Haddad 2008). The borders and blocks that are constrained by faults may be seen in the structural sections. Hence, the seismic boundaries and faults may be assigned to these images. The transition zones with the highest lighting (brighter lines) are where the velocity rises with depth and the inversion discontinuities with the lowest illumination or dark lines.

The 2D velocity models for the nine identified profiles on the hypothetical expansion of the Spillway Fault were created by processing and interpreting the seismic data acquired in the examined locations using the 2D tomographic inversion method (GODOGRAF software), as illustrated in Figs. 5, 6, 7, 8, 9, 10, 11, 12 and 13 Up. These models are shown as fields of contour lines representing velocity with an interval of 1000 m/sec. Given that the gradient is inversely proportional to the separation between contours, it is feasible to visually estimate the velocity gradient values from these lines. The seismic zones, which may act as the strata, can be delineated by extended boundaries and maintaining the values of the velocity gradient and velocity interval from top to bottom of strata (Piip 2001; Piip and El-Haddad 2008). Moreover, Figs. 5, 6, 7, 8, 9, 10, 11, 12 and 13 Down show the structural sections for the same nine profiles that were scattered throughout the study locations. the same velocity pattern is shown as a surface with a shaded relief and velocity contour
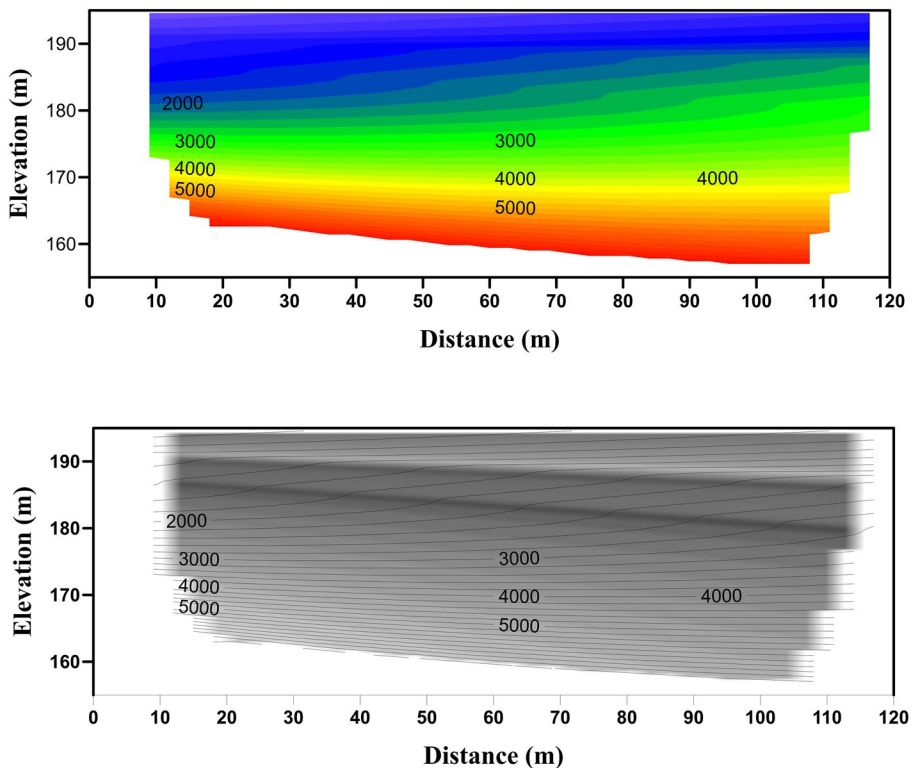

Fig. 5 Seismic velocity section along profile No.1. (Up) The 2-D velocity section, and (Down) Structural section (the P-wave velocity in m/s)
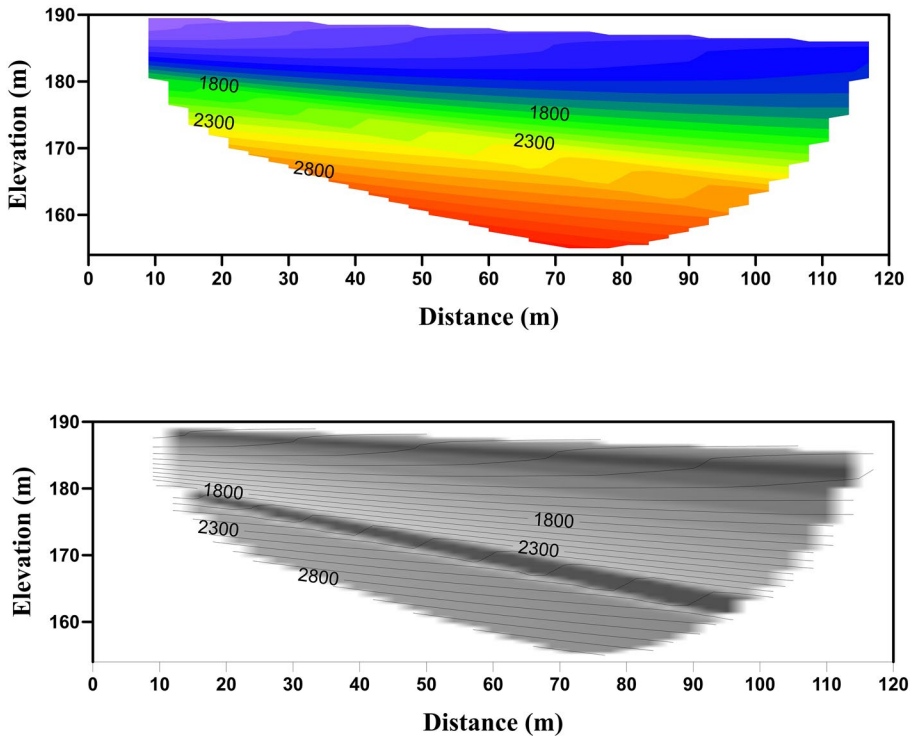
Profile (2)

Fig. 6 Seismic velocity section along profile No.2. (Up) The 2-D velocity section, and (Down) Structural section (the P-wave velocity in m/s)

isolines overlaid on it. The borders and blocks that are constrained by faults may be seen in the structural sections. Therefore, the seismic boundaries and faults may be assigned to these images.

3.2 Multi-channel analysis of surface waves (MASW)

Geophones are arranged in a straight line on the test site's surface to collect MASW data. As a seismic geophysical method, the MASW methodology can be used, and it is crucial that they are positioned vertically on the ground to estimate the soil shear wave velocity profile. It was introduced in the late 1990s as a development of existing surface wave methods (Park et al. 1999; Nazarian 1984; Ballard Jr 1964). This method has been used for several purposes, including the assessment of seismic sites in accordance with building codes and, the calculation of dynamic soil parameters and conditions before and after construction (Fat-helbary et al. 2019a, b; Abodeif et al. 2019a, b; Al-Heety et al. 2021), and the identification of subterranean cavities (Xia et al. 2006a, b; Abbas et al. 2023). The longest wavelength of a surface wave that is acquired during data collection determines the maximum investigation depth. A widely used empirical criterion according to Park and Carnavele (2010) is that:
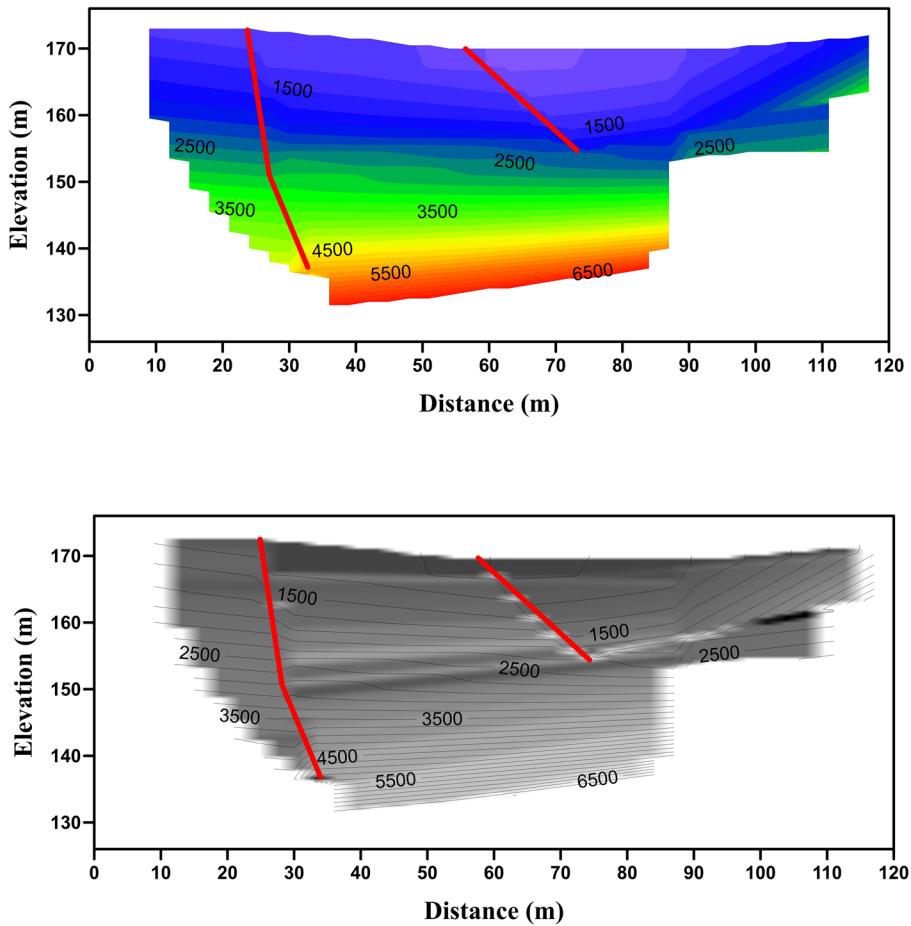
Profile (3)

Fig. 7 Seismic velocity section along profile No.3. (Up) The 2-D velocity section, and (Down) Structural section (the P-wave velocity in m/s and the red line represents fault)

$$Z_{max} \approx 0.5\lambda_{max} \tag{1}$$

In a broad sense, the investigative depth will progressively increase as the seismic source becomes stronger. A relatively heavy sledgehammer is a popular option (e.g. 10 kg). Additionally, the use of an impact plate metallic or non-metallic can assist in the generation of surface waves characterized by low frequency and long wavelength Park et al. (2002). The greatest depth of study is correlated with the receiver spread's length (L), which is proportional to the longest wavelength that may be generated.

$$\lambda_{max} \approx L \tag{2}$$

The empirical requirements for the greatest depth of investigation previously stated can be described in terms of the receiver spread's length as follows:
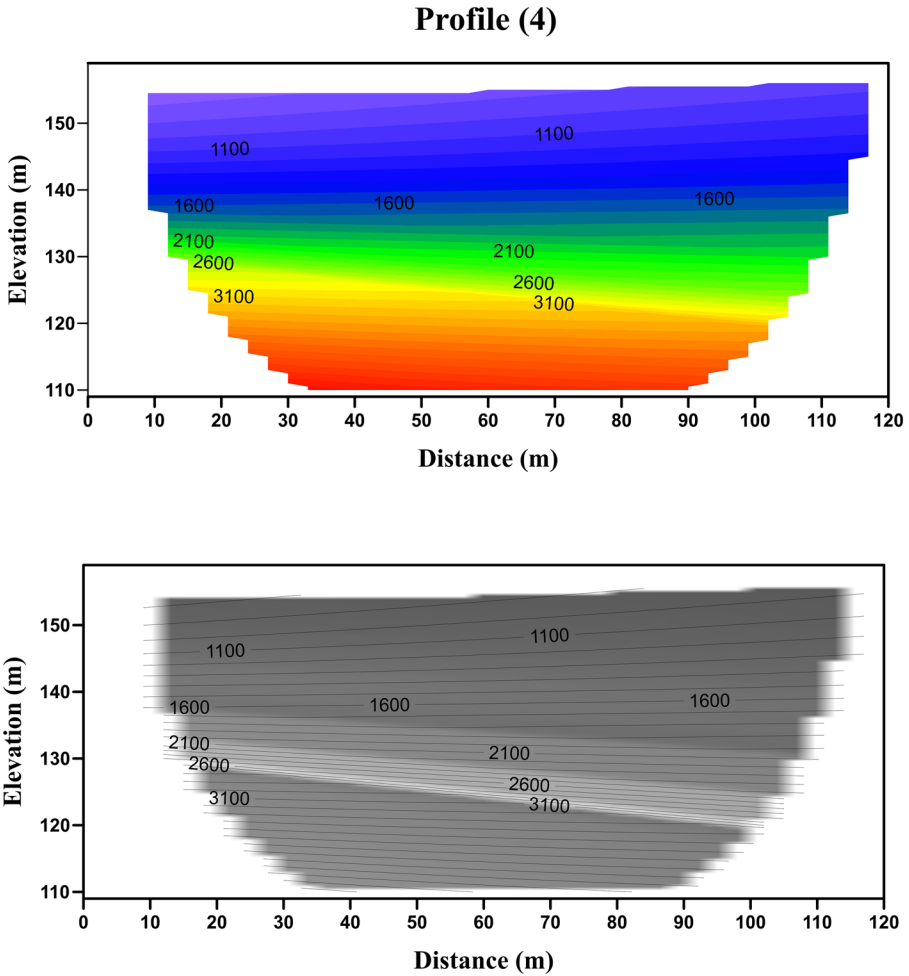
Profile (4)

Fig. 8 Seismic velocity section along profile No.4 (Up) The 2-D velocity section, and (Down) Structural section (the P-wave velocity in m/s)

$$Z_{max} \approx 0.5L \tag{3}$$

However, an extremely wide receiver spread should be avoided. At the end of an unusually long receiver spread. Surface waves could have attenuated underneath the noise level, making the signal from the most distant geophones too noisy to be useful (Park et al. 1999). In order to determine the shallowest resolvable depth of examination, the shortest wavelength that may be investigated (z_{min}) is linked to the geophone spacing (dx).

$$dx = n.z_{min} \tag{4}$$

where $0.3 \leq n \leq 1.0$

The separation between the source and nearest receiver is known as "source offset," and it is represented by (x_1). Unwanted near-field effects can be reduced by adjusting the source
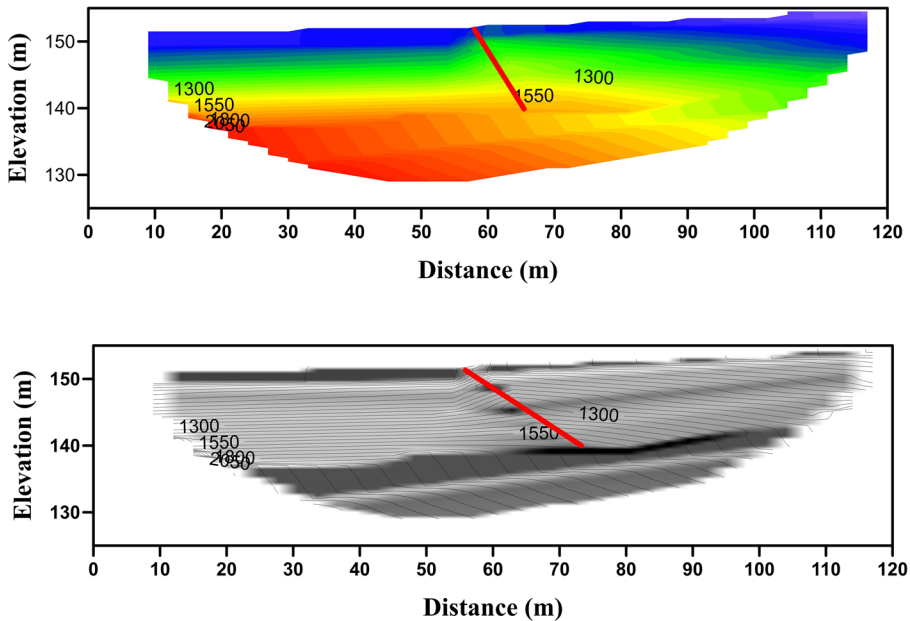
Profile (5)

Fig. 9 Seismic velocity section along profile No.5 (Up) The 2-D velocity section, and (Down) Structural section (the P-wave velocity in m/s and the red line represents fault)

offset for a specific measurement profile (Park and Carnavare 2010). According to some reports, a long source offset (x_1), might increase energy for long wavelengths i.e. reach to deeper strata (Park and Shawver 2009; Park and Carnavare 2010). Therefore, it has been stated that the lowest and highest source offsets are as follows:

$$x_{1.\,\text{min}} = 0.2L \text{ and } x_{1.\,\text{max}} = L \tag{5}$$

In order to raise the amplitudes of consistent surface wave signals and to increase the signal-to-noise ratio (S/N) as a way to overcome noisy environments, successive repeated hits and the recorded data can be stacked together (Ivanov et al. 2008).

A data-gathering device is attached to the geophones. Geophones with low frequencies, such as 4.5 Hz, are advised. Typically, 12 or more geophones are employed, each of which is linked to a different recording channel (Park et al. 1997). 24 or 48 receivers are frequently employed in reported studies (Park and Carnevale 2010; Donohue et al. 2013). In general, a better resolution in the dispersion image may be obtained by using more geophones for recordings (Park et al. 2001). Equal distance between the receivers should be used (Park et al. 1997). Figure 14 displays the basic measurement profile for a 24-geophone active MASW survey.

An impulsive seismic source with a total time of recording (T) of approximately one and a half seconds and a sampling interval of one millisecond was used for the MASW survey. The greatest depth of investigation (z_{max}) is affected by the type of seismic origin employed and the investigated site. Appropriately heavy sledgehammer (such as 10 kg) is
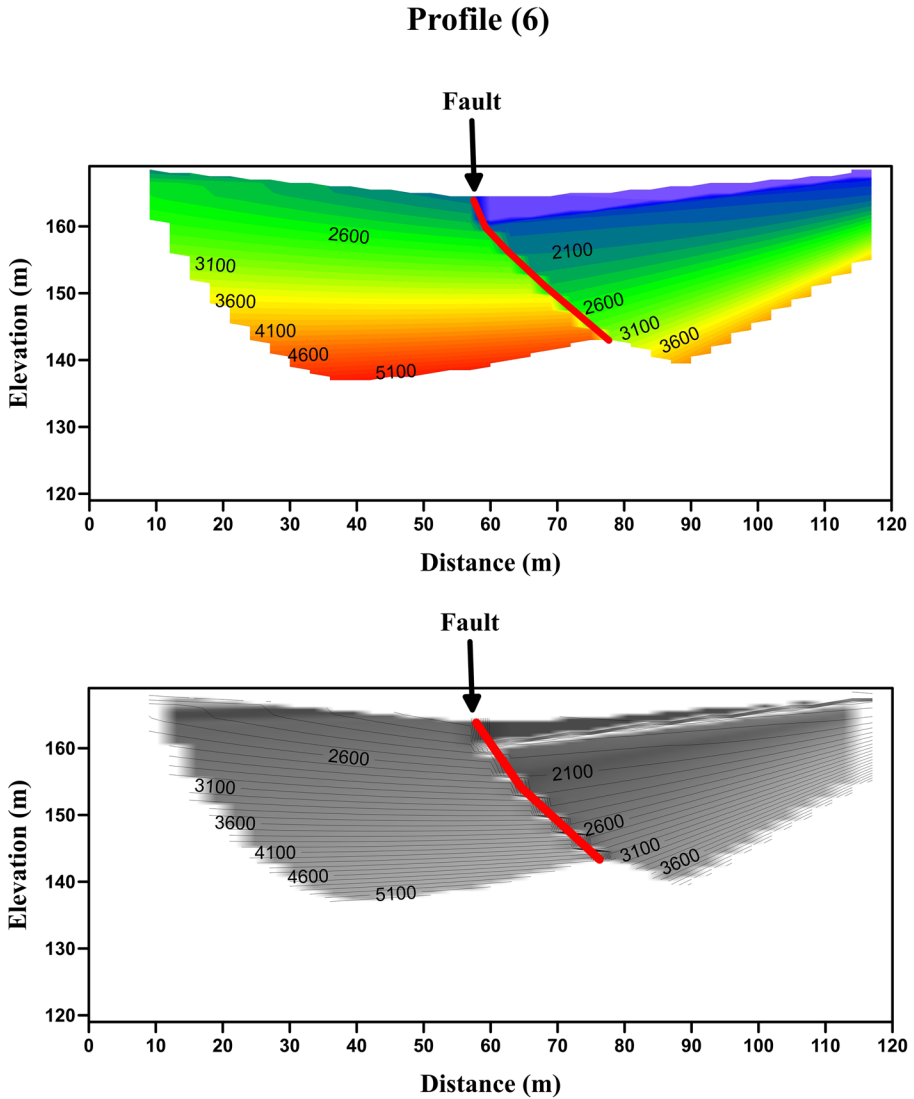
Profile (6)

Fault

Fault

Fig. 10 Seismic velocity section along profile No.6 (Up) The 2-D velocity section, and (Down) Structural section (the P-wave velocity in m/s and the red line represents fault)

a common alternative. Using an impact plate (base plate) can also help to produce low-frequency surface waves.

During the survey planning, 17 locations have been chosen for the acquisition of surface-wave data (Fig. 14a). Seismic data are collected by using Geometrics StrataVisor NZ seismograph. For surface waves with frequencies as low as 4 Hz, 24 low-frequency (4.5 Hz) vertical component geophones are widely applied, allowing for maximum investigation depths of more than 30 m for the majority of studied points (Park et al. 2001), the geophones were spaced 2 m apart (Park et al. 1997). The energy source for surface-wave
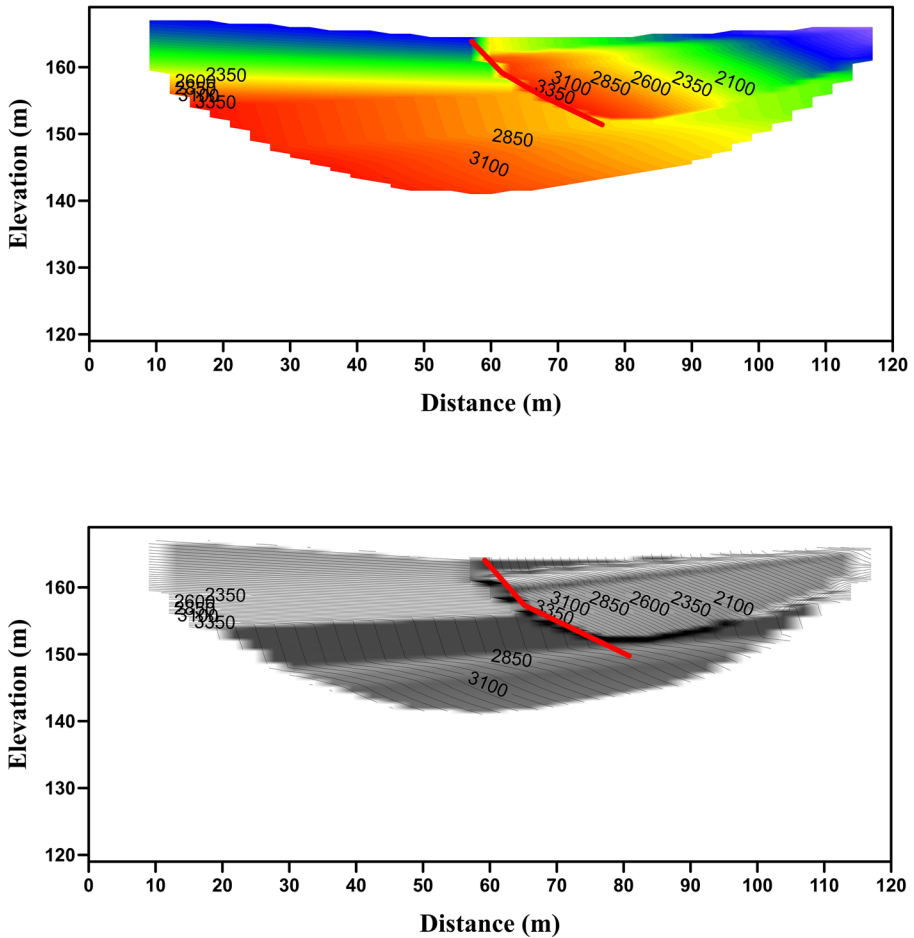
Profile (7)

Fig. 11 Seismic velocity section along profile No.7 (Up) The 2-D velocity section, and (Down) Structural section (the P-wave velocity in m/s and the red line represents fault)

generation was a vertical strike from a 10-kg sledgehammer. On all recordings, a stacking technique was used with a total of five stacks to boost the signal-to-noise ratio (S/N) (Ivanov et al. 2008). In order to optimize and restrict the data inversion and confirm the validity of the seismic velocity spectrum, the offset (x_1) was adjusted at 5 m and 10 m at the normal and reverse sides of each profile (Fig. 14b) in order to improve the obtained dispersion curve by allowing monitoring of the near- and far-field effects (Park et al. 2001; Yoon and Rix 2009). In this study, a fixed source-receiver layout has been used (Fig. 14b). All of the shot gathers have been merged into a single file, pre-processing, picking, and inversion were done to data (Fig. 15a). Depending on the positions of the source and receivers, and the spacing between the geophones, field geometry is then applied to the
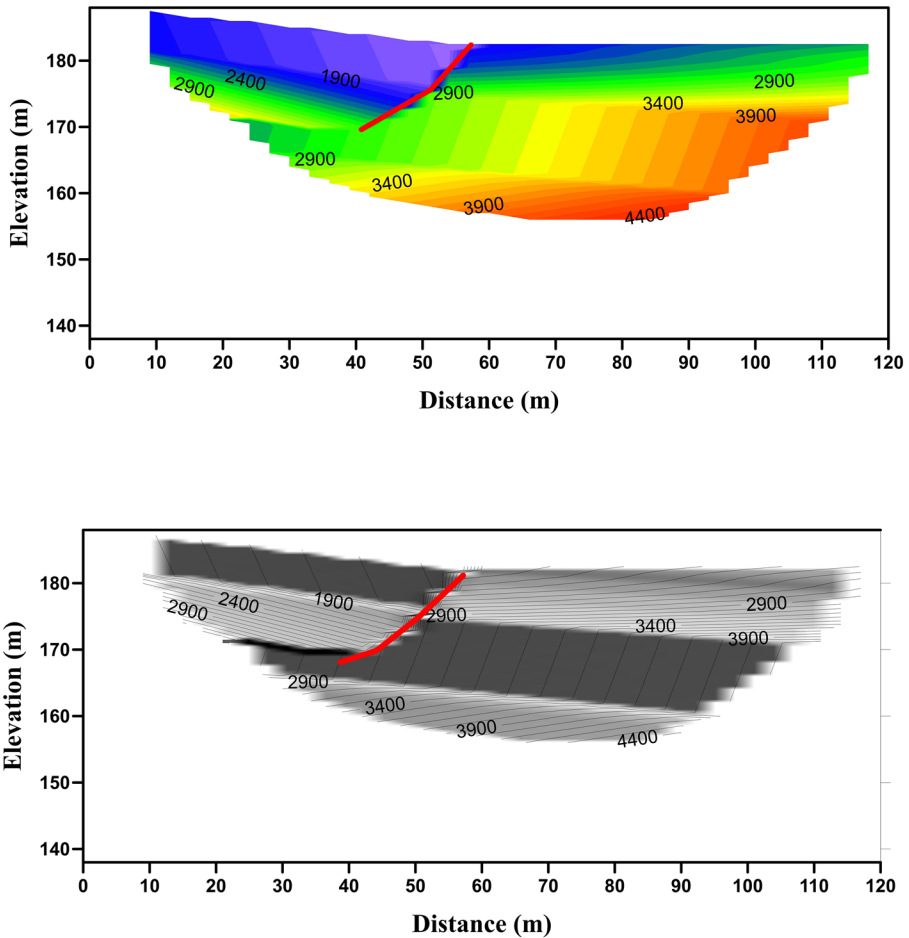
Profile (8)

Fig. 12 Seismic velocity section along profile No.8(Up) The 2-D velocity section, and (Down) Structural section (the P-wave velocity in m/s and the red line represents fault)

data. In addition, it should establish a common frequency range for all inputs and define the frequency ranges of surface-wave signals shot by shot.

Additionally, to eliminate back scattering and remove the higher mode effect, the *f-k* filter should be applied to the raw data (Fig. 15b). In addition, to alleviate some of the interference on the fundamental mode, the higher mode was chosen and employed in the dispersion-curve *f-k* filter to eliminate high-velocity surface wave energy between 65 and 75 Hz (Morton et al. 2015). In comparison to the original data, the fundamental mode energy became more prominent after passes in the filtered traces. This filter is applied to shot gathers to increase the signal-to-noise ratio required by surface-wave analysis. This large ratio indicates that the derived phase velocity-frequency curve may be accepted (Fig. 15c).
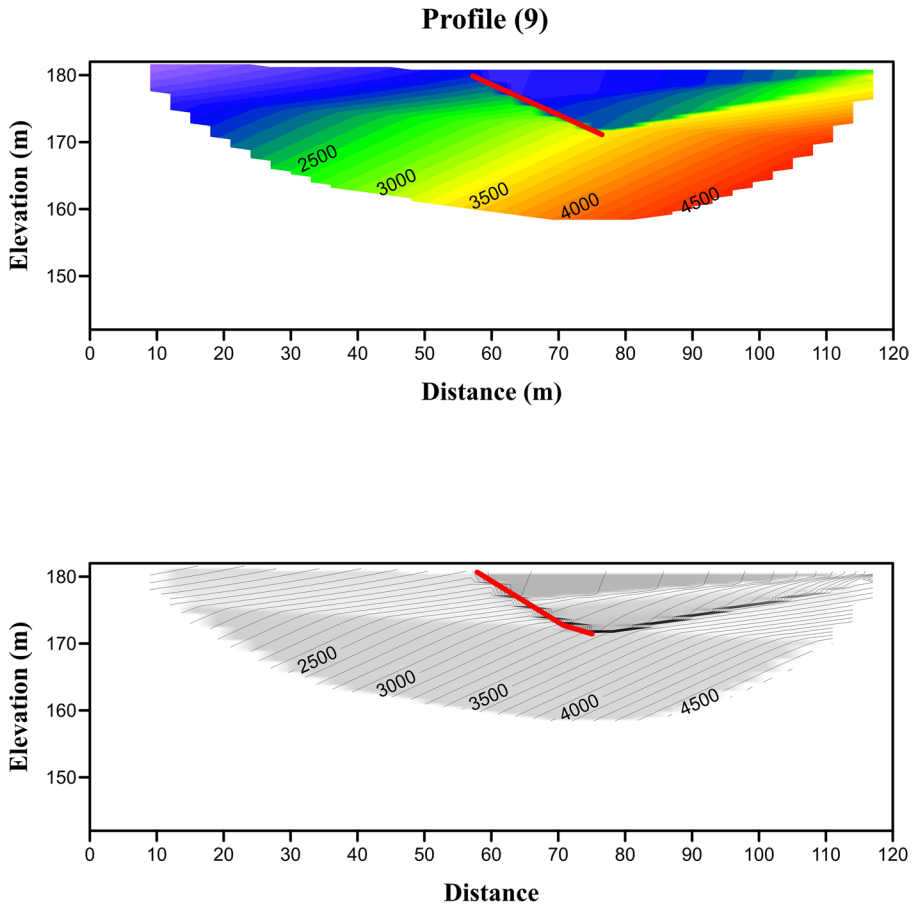
Profile (9)

Fig. 13 Seismic velocity section along profile No.9 (Up) The 2-D velocity section, and (Down) Structural section (the P-wave velocity in m/s and the red line represents fault)

The phase velocities-frequency dispersion curve of the fundamental mode was manually picked from 6 to 63 Hz. The input signal for inversion is derived from the surface wave's fundamental mode. The fundamental mode is always the most prevailing one (Taipodia et al. 2012), however, this is not often the ideal case. Poor picks and the miss-identification of different modes will give unreasonable outcomes. Following every iteration, the shear wave velocity is modified, and the inversion method starts by looking for a Vs profile whose theoretical dispersion curve matches the experimental dispersion curve acquired from the dispersion examination. If there is no matching, the inversion will change the Vs profile, and the process will be repeated by calculating a new theoretical curve. Iterations refer to each cycle of this search; they keep going until a matching occurs and a low root mean square error is attained (Park et al. 1999). As a result, material that lies right under the center of the geophones spread will yield a 1D profile that is most representational of it (Fig. 15d).

The precise extraction of the dispersion curve is based on the exact interpretation of the subsurface geology (Park and Miller 2001). The 1D shear wave velocity models have
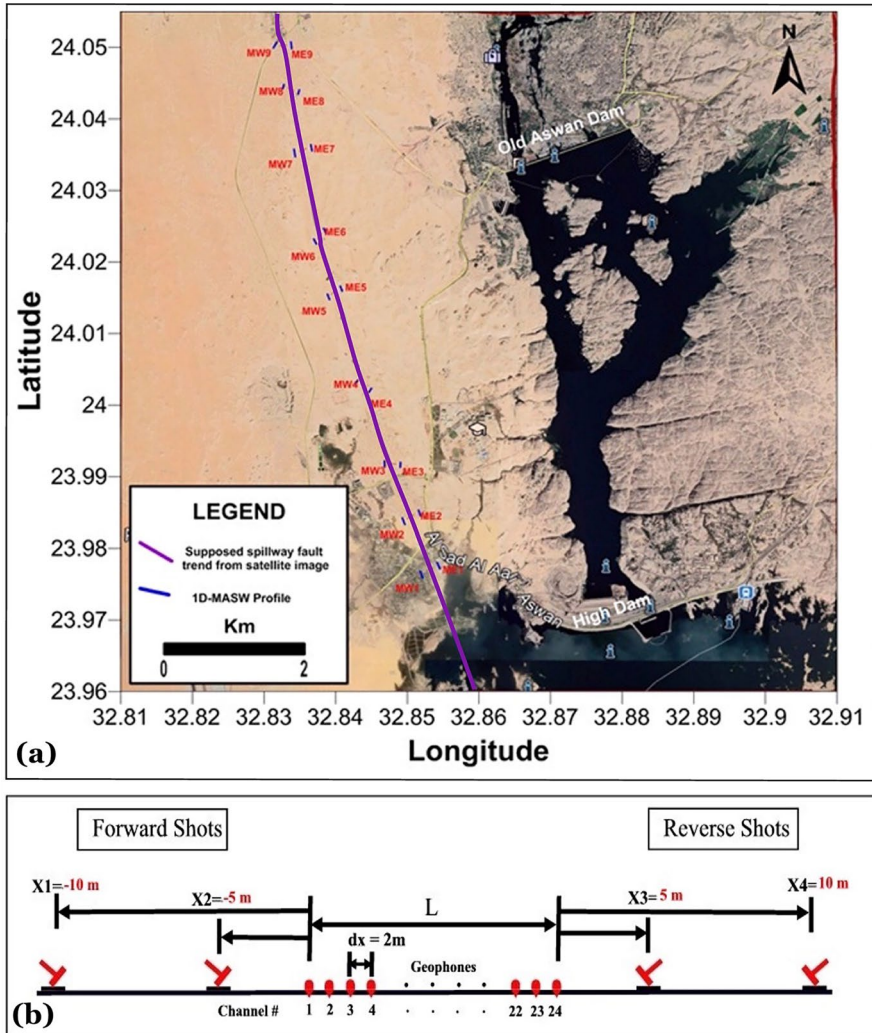
Fig. 14 Location map of the seismic MASW profiles around supposed Spillway fault (**a**), the Source-Receiver configuration with a standard fixed roll along for 1D MASW field survey (**b**)

several striking features likely affected by changes in material properties or lithology. Variations in material textures, cementation, or compaction are probably related to rapid changes in the velocity gradient. Data possessed a usable bandwidth of 6 to 63 Hz, equating to a depth of penetration of more than 30 m. In consequence, Fig. 16 has been constructed to display the variation in shear wave velocity values around the expected Spillway Fault at different depths. The 1D shear wave velocity models have several striking features likely affected by changes in material properties or lithology. Variations in material textures, cementation, or compaction are probably related to rapid changes in the velocity gradient.
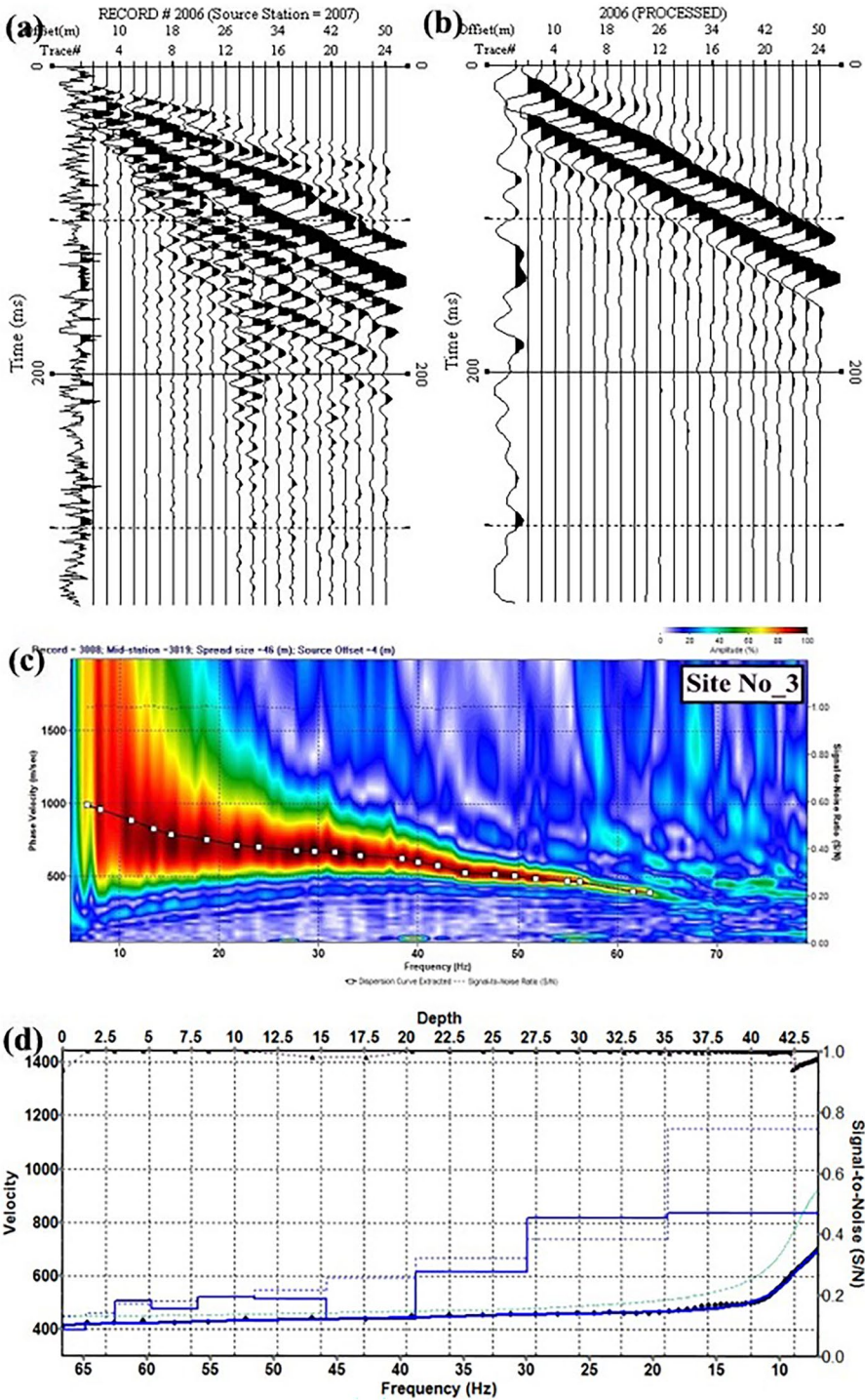
Fig. 15 MASW raw data records (**a**), applying of the *f-k* filtering (**b**), The dispersion curve deduced from the surface wave records (**c**), 1D shear wave velocity model (**d**)
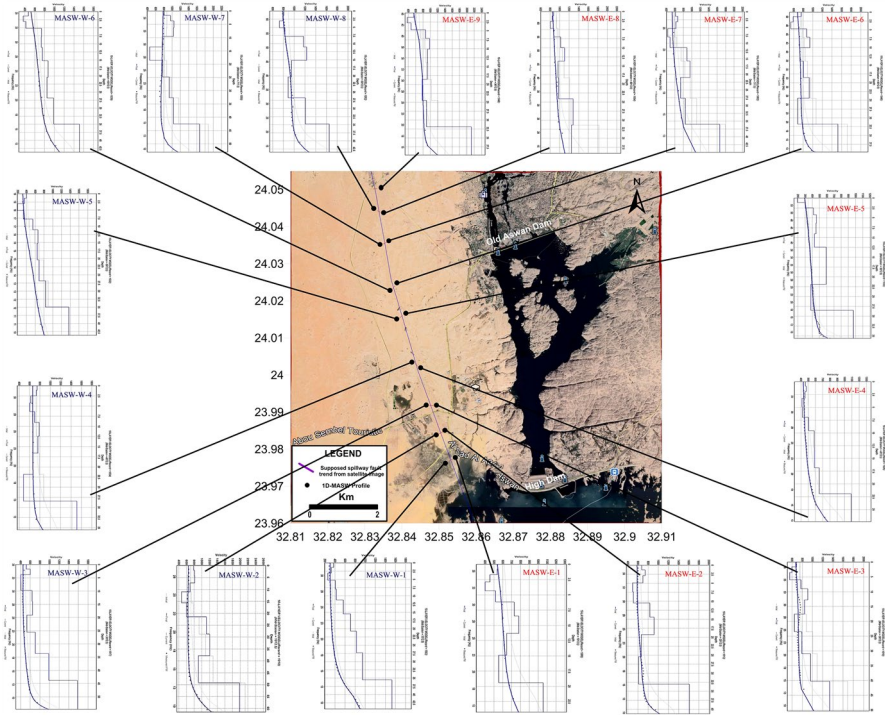
Fig. 16. 1D Vs model obtained for all profiles along the two sides of the supposed Spillway Fault trace

3.3 Vs30 site classification

In general, several factors, such as the near-surface geology, source characteristics, and seismic wave spreading pathway, influence ground motion. In earthquake and civil engineering, the elastic properties of materials close to the surface and their influence on seismic wave penetration are particularly important. One of the most significant variables contributing to the amplifying of earthquake movements is the rise of amplitudes in soft or loose sediments (First et al. 2015). The amplification of seismic waves is inversely proportional to the outcome of the shear wave velocity (Vs) and the observed soil density (ρ) and is strongly correlated with regions having a significant impedance contrast (Aki and Richards 2002):

$$A \propto \frac{1}{\sqrt{V_s \rho}} \tag{6}$$

where the density of the soil under investigation is (ρ) and (Vs) is the shear wave velocity, the Vs profile more accurately captures the site conditions in the area. Recently, it has been able to determine the soil characteristics of the research region as well as the shear wave velocities (Vs) using the MASW approach. We can analyze the shear wave velocity (Vs) and soil properties of the area near the suggested Spillway Fault extension up to a depth of

Table 3 Vs30 and sites classes according to NEHRP site classification

Profie	Eastern profiles	Vs30	Site class	Western profiles	Vs30	Site class
1	E-1	761	B	W-1	542	C
2	E-2	664	C	W-2	711	C
3	E-3	762	B	W-3	548	C
4	E-4	627	C	W-4	672	C
5	E-5	443	C	W-5	483	C
6	E-6	772	B	W-6	698	C
7	E-7	685	C	W-7	774	B
8	E-8	955	B	W-8	961	B
9	E-9	775	B	W-9	–	–

30 m, The following equation should be used to determine the average shear wave velocity of the top 30 m (Vs30):

$$Vs30 = \frac{30}{\sum_{i=1}^{N} (\frac{h_i}{v_i})} \tag{7}$$

According to Eq. (7), (*i*th) denotes a formation or layer that is located in the top 30 m, and (h_i) and (v_i) stand for the formation or layer's thickness (in meters) and shear wave velocity, respectively. The NEHRP Code accepted Vs 30 for site categorization (Table 2). The computed Vs30's value and categorization for each profile are shown in Table 3 in accordance with the differences in shear wave velocities with depth. The research area's topsoil is divided into two categories, B and C.

4 Results and discussion

The seismic refraction and the multichannel analysis of surface waves (MASW) methods have become more familiar due to their low-cost, environment-gently, non-destructive, and effective outputs. This paper clarified a case study of conducting integration of seismic refraction and MASW methods for the supposed Spillway Fault investigation in the Aswan High Dam area. For detecting the fault trace, nine seismic refraction profiles crossing the fault and seventeen MASW lines along both sides of the supposed fault trace were implemented. The main purposes of combining seismic refraction and MASW methods were to minimize the uncertainty and confirm the obtained results.

Processing of the obtained seismic refraction profiles is represented in 2D velocity models. Accordingly, the above-mentioned criteria indicate that the P-wave's greatest penetration, as seen in profiles 3 and 4, reached 40 and 50 m, respectively (Figs. 7 and 8). Additionally, the obtained P-wave velocities in the research locations range from less than 600 m/sec to more than 6500 m/sec. The distribution of those different velocities makes it appear as though a strong anisotropic medium exists in each of the vertical and lateral directions of the analyzed subsurface areas. Seismic zones may be created by dividing the seismic velocity variation range into smaller sections and preserving the values of the velocity gradient and velocity interval from top to bottom. The produced 2D seismic

velocity and structural sections along the nine observed profiles in the Spillway Fault area also demonstrate that the seismic wave velocities throughout the nine profiles rise with depth and their variance spans from less than 600 to more than 6500 m/s. Seismic wave velocities show some lateral change across all strata at profile 6 (Fig. 10); these lateral changes may correspond to fault zones, whereas for profiles 3, 5, 6, 7, 8, and 9 (Figs. 7, 9, 10, 11, 12 and 13) the first layer's horizontal differences are obvious that might be cracks or fractions brought on by the nearby Spillway Fault. There is no lateral variation in the seismic wave velocities detected at profiles 1, 2, and 4, it could be a result of the passage of high-pressure lines of electricity above the places of the profiles, which affected the geophones and worked on the seismic waves, which made it difficult to determine the onset of the seismic wave signals correctly, or may those profiles not crossed correctly the supposed Spillway Fault.

On the other hand, the 1D shear wave velocity models have several striking features likely affected by changes in material properties or lithology. Variations in material textures, cementation, or compaction are probably related to rapid changes in the velocity gradient. Figure 16 shows 1D shear wave velocity models located around the supposed Spillway Fault trace. The general impression that could be taken from those models is that Vs values for most of the layers on the western side are lower, while most of the profiles at the eastern side layers show high shear wave velocity values, this phenomenon could be interpreted as the existence of normal dip-slip fault or fraction and fissure due to this fault running between the profiles.

In addition, as seen in Table 3, Vs30 values which were deduced from the analysis of the shear wave profiles emphasized the idea of the occurrence of a local dip-slip fault affecting the study area and divided it into two different lithological parts; the first part which located in the eastern part characterized by almost class B (rock site, according to NEHRP classification), while the second part which located to the west shows almost class type C (denoted as dense soil and soft rock soil). The calculated Vs30 value showed that the soil of the study area is classified into two groups B and C which confirmed the existence of a local dip-slip fault.

5 Conclusion

In the framework of an applied multidisciplinary geophysical survey at a chosen study area, two inexpensive seismic methods were applied. Thus, in order to image and identify the spillway Fault track, seismic refraction and multichannel analysis of surface waves (MASW) were conducted. According to the seismic refraction profiles, we can notice that the detected fault caused relatively considerable displacement in the sedimentary and basement rocks, this obtained result coincides with the obtained cross-section obtained (WCC 1985). In addition, the 1D shear wave velocity models derived from the MASW approach exhibit several characteristics influenced by material property changes brought about by abrupt variations in the velocity gradient along the western and eastern sides of the assumed Spillway Fault path. Consequently, the Vs and the Vs30 values for most of the layers on the western side are lower and have soil class type C. According to the soil classification system, the majority of the profiles on the eastern side exhibit high shear wave velocity layers and B-type soil. These findings might be taken as evidence of a typical dip-slip fault that affects the research region and divides it into two distinct lithological portions. In conclusion, we could say that the promising outcomes of this case study

indicate that the combination of MASW and seismic refraction methods has a significant contribution to investigating faults at shallow depths.

Declarations

Conflict of interest The authors declare no conflict of interest. The funders had no role in the design of the study; in the collection, analyses, or interpretation of data; in the writing of the manuscript; or in the decision to publish the results.

References

Abbas MA, Fat-Helbary R ES, Hamed A, El-Faragawy K O, El-AminE M, El-Qady GM (2023) The Implementation of ShallowGeophysical Survey for Detection of Some Buried ArchaeologicalStructures in Aswan City, Egypt. SustainableConservation of UNESCO and Other Heritage Sites Through Proactive Geosciences, Springer Geology. https://doi.org/10.1007/978-3-031-13810-2_11

Abudeif AM, Fat-Helbary RE, Mohammed MA, Alkhashab HM, Masoud MM (2019a) Geotechnical engineering evaluation of soil utilizing 2D multichannel analysis of surface waves (MASW) technique in New Akhmim city, Sohag, Upper Egypt. J African Earth Sci 157:103512

Abudeif AM, Fat-Helbary RE, Mohammed MA, Alkhashab HM, Masoud MM (2019b) Geotechnical engineering evaluation of soil utilizing 2D multichannel analysis of surface waves (MASW) technique in New Akhmim city, Sohag, Upper Egypt. J Afr Earth Sci. 157

Adeoti L, Alile OM, Uchegbulam O, Adegbola RB (2012) Seismic refraction prospecting for groundwater: a case study of Golden Heritage Estate, Ogun State. Res J Phys 6:1–18

Aki K, Richards PG (2002) Quantitative seismology, 2nd edn. University Science Books, Sausalito

Al-Heety AJ, Hassouneh M, Abdullah FM (2021) Application of MASW and ERT methods for geotechnical site characterization: a case study for roads construction and infrastructure assessment in Abu Dhabi, UAE. J Appl Geophys, 193

Al-Heety AJ, Shanshal ZM (2016) Integration of seismic refraction tomography and electrical resistivity tomography in engineering geophysics for soil characterization. Arab J Geosci 9(1):1–11

Attia MI (1955) Topography, geology and iron ore deposits of east aswan: Geol. Survey, Egypt, Cairo, Internal Report

Ballard RF (1964) Determination of soil shear moduli at depths by in-situ vibratory techniques; U.S. Army Engineer Waterways Experiment Station, Engineer Research and Development Center, Vicksburg, MS, USA

Bessason B, Erlingsson S (2011) Shear wave velocity in surface sediments. Jökull 61:51–64

Burger H.R., Sheehan AF, Jones CH (2006) Introduction to applied geophysics—exploring the shallow subsurface. WW Norton and Company

Butler DK (1990) Seismic refraction tests above the water table. Geotech Eng 116(9):1434–1436

Woodward-Clyde Consultants (1985) Earthquake activity and dam stability evaluations for the Aswan High Dam, Egypt, vol 3: seismic geology and tectonic studies of the Aswan Region, report to High Aswan Dam

Dahy SA (2012) A study on shallow and deep focus earthquakes and relationship to the water level in the western side of the Aswan High Dam Lake, Egypt. Res J Earth Sci 4(2):63–68. https://doi.org/10.5829/idosi.rjes.2012.4.2.6377

Donohue S, Dermot F, Donohue LA (2013) Detection of soil compaction using seismic surface waves. Soil Tillage Res 128:54–60

Egyptian Geological Survey and Mining Authority (2002) A geological map of Assiut Area, scale 1:100,000

El-Bohoty M, Ghamry E, Hamed A, Khalifa M, Taha A, Meneisy A (2023) Surface and subsurface structural mapping for delineating the active spillway fault, Aswan, Egypt, using integrated geophysical data. Journal Acta Geophysica (In press)

Fat-Helbary RE, El-Faragawy KO, Hamed A (2019a) Application of HVSR technique in the site effects estimation at the South of Marsa Alam City, Egypt. J African Earth Sci 154:89–100. https://doi.org/10.1016/j.jafrearsci.2019.03.015

Fat-Helbary RES, El-Faragawy KO, Hamed A (2019) Soil geotechnical characteristics for seismic risk mitigation at the southern extension of Marsa Alam city, Egypt. NRIAG J Astron Geophy 8(1):1–14

Fat-Helbary RE, Hassib GH, Mohamed HH, Taha YS, Mostafa SM, Abdel-motaal A, Elamin EM, Hamed A. (2012) Investigation of the November 7, 2010 Aswan Earthquake, Egypt. Seventh Gulf Seismic Forum, Jeddah, Saudi Arabia

First S, Isik NS, Arman H, Demir M, Vural I (2015) Investigation of the soil amplification factor in the Adapazari Region. Bull Eng Geol Environ 75:141–152

Hamed A, Fat-Helbary RE, Mohamed EM, El-Faragawy KO (2023) Seismic site characteristics for geotechnical engineering purposes: case study, South of Ras Samadai, Red Sea, Egypt. J Appl Geophys. https://doi.org/10.1016/j.jappgeo.2023.105223

Hamed A (2019) Seismic Microzonation for earthquake risk mitigation at the southern extension of Marsa Alam City. Ph.D.'s Thesis. Aswan University, Aswan, Egypt

Hendriks F, Luger P, Bowitz J, Kallenbach H (1987) Evolution of the depositional environments of SE-Egypt during the Cretaceous and Lower Tertiary. Berliner geowissAbh (a) 75(1):49–82

Holzer TL, Bennett MJ (2003) Unsaturated beneath a water table. Environ Eng Geosci 9(4):379–385

Ivanov J, Miller RD, Tsoflias G (2008) Some practical aspects of MASW analysis and processing: symposium on the application of geophysics to engineering and environmental problems, 21, 1186–1198.

Karastathis VK, Ganas A, Makris J, Papoulia J, Dafnis P, Gerolymatou E, Drakatos G (2006) The application of shallow seismic techniques in the study of active faults: the atalanti normal fault, central Greece. J Appl Geophys 62(2007):215–233. https://doi.org/10.1016/j.jappgeo.2006.11.004

Kearey P, Brooks M, Hill I (2002) An introduction to geophysical exploration, 3rd edn. Blackwell Science Ltd, Oxford, p 281

Meneisy AM, Toni M, Omran AA (2020) Soft sediment characterization using seismic techniques at Beni Suef City, Egypt. J Environ Eng Geophys 25(3):391–401

Meneisy AM, Hamed A, Khalifa M, El-Bohoty M, Ghamry E, Taha A (2023) Geotechnical Zonation and Vs30 classification of soil for seismic site effects evaluation in the western extension of New Aswan City. Egypt Pure Appl Geophys 180:3813–3833. https://doi.org/10.1007/s00024-023-03370-3

Mohamed AS, Hassib GH, AbouAly N, El-Kutb A (2022) Evaluation of recent crustal deformation and seismicity in spillway fault area, Aswan, Egypt NRIAG. J Astron Geophys. https://doi.org/10.1080/20909977.2022.2106667

Morton S LC, Peterie S, Livers A, Ivanov J, Miller RD (2015) Advantages and disadvantages of passive multichannel analysis of surface waves (MASW) of observing subsurface discontinuities, American geophysical union, fall meeting 2015, Abstract id. NS41A-1921

Nazarian S (1984) In situ determination of elastic moduli of soil deposits and pavement systems by spectral-analysis-of-surfacewaves method; the national academies of sciences, engineering, and medicine. Washington, USA

NEHRP (2004) For seismic regulations for new buildings and other structures (FEMA450) 2003 Edition, Part 1. Provisions, building safety council for the federal emergency management agency, national institute of building sciences, Washington

Park CB, Miller RD, Xia J (1998) Imaging dispersion curves of surface waves on multichannel record: technical program with biographies, SEG, 68th annual meeting. Louisiana, New Orleans, pp 1377–1380

Park CB, Carnevale M (2010) Optimum MASW survey—revisit after a Decade of Use. In: Fratta DO, Puppala AJ, Muhunthan B (eds) GeoFlorida 2010: Advances in analysis, modeling and design (pp. 1303–1312). https://doi.org/10.1061/41095(365)130

Park CB, Miller RD (2001) Offset and resolution of dispersion curve in multichannel analysis of surface waves (MASW). Proceedings of the SAGEEP Conference

Park CB, Shawver JB (2009) Multi-source offset MASW survey. In: Proceedings of the symposium on the application of geophysics to engineering and environmental problems (SAGEEP 2009), Fort Worth, Texas

Park CS, Marx GD, Moon YS, Wiesenborn D, Chang KC, Hofman VL (1997) Alternative uses of sunflower. In: Schneiter AA (ed) Sunflower technology and production. Agronomy monograph no. 35. ASA, CSSA, SSSA, Madison, Wisconsin, pp765–807

Park CB, Miller RD, Xia J (1999) Multichannel analysis of surface waves (MASW): Geophysics, 64: 800–808

Park CB, Miller RD, Miura H (2002) Optimum field parameters of an MASWsurvey. Expanded Abstracts, SEG-J, Tokyo

Piip VB (1991) Local reconstruction of seismic refraction sections on the basis of homogeneous functions. Izvestiya. Acad Sci USSR Phys Solid Earth v 27:844–850

Piip VB (2001) 2D inversion of refraction traveltime curves using homogeneous functions. Geophys Prospect 49:461–548

Piip VB, El- Haddad AE (2008) Automatic interpretation of shallow seismic data with homogeneous function method to investigate landslide body of Dallackau area, northern OssetiyaAllaniya. Russia J Appl Geophys 7(1):321–337

Rahnema H, Ehsaninezhad L, Dashti F, Talebi G (2020) Detection of subterranean cavities and anomalies using multichannel analysis of surface wave. Geomech Geoeng 1–14

Rasif N, Rachman AA, Mariyanto M (2023) Identification of shallow fault with seismic refraction modelling in gondang area, Bojonegoro. In: IOP Conference series: earth and environmental science. https://doi.org/10.1088/1755-315/1227/1/012006

Taipodia, Jumrik , Dey, Arinada (2012) A Review of Active and Passive MASW Techniques: EGCEG, CBRI, Roorkee.

Toni M, Yokoi T, El Rayess M (2019) Site characterization using passive seismic techniques: a case of Suez City, Egypt. J African Earth Sci 156(2019):1–11. https://doi.org/10.1016/j.jafrearsci.2019.05.004

Toni M, El Rayess M, Hafiez HA (2022) Local site characteristics and earthquake ground motion parameters around the Nile River, south of Cairo, Egypt. J Appl Geophys 197:104528

Toni M (2012) Site response and seismic hazard assessment for the southern part of Cairo city, Egypt. PhD dissertation, Faculty of Science, Assiut University, Egypt

Xia J, Miller RD, Park CB (1999a) Estimation of near surface velocity by inversion of Rayleigh wave. Geophysics 64:691–700

Xia J, Miller RD, Park CB (1999b) Estimation of near surface shear-wave velocity by inversion of Rayleigh waves. Geophysics 64(3):691–700

Xia J, Miller RD, Park C, Tian G (2002) Inversion of high frequency surface waves with fundamental and higher modes. J Appl Geophys 52:45–57

Xia J, Xu Y, Chen C (2006a) Simple equations guide high-frequency surface-wave investigation techniques. Soil Dyn Earthq Eng 26(5):395–403

Xia J, Xu Y, Miller RD (2006b) Estimation of elastic moduli in a compressiblegibson half-space by inverting Rayleigh wave phase velocity. Surv Geophys 27(1):1–17

Yoon S, Rix GJ (2009) Near-field effects on array-based surface wave methods with active sources. J Geotech GeoenvironEng 135:399–406

Youssef MM (2003) Structural setting of central and south Egypt: an overview. Micropaleontology 49:1–13